

# A Stacked Dual-Active-Half-Bridge DC/DC Differential Power Converter

Matthew Jahnes  
Electrical Engineering  
Columbia University  
New York City, USA  
matthew.jahnes@columbia.edu

Matthias Preindl  
Electrical Engineering  
Columbia University  
New York City, USA  
matthias.preindl@columbia.edu

**Abstract**—This brief discusses a DC/DC converter implemented as a Dual-Active-Half-Bridge (DAHB) that has been folded across its galvanic isolation and stacked upon itself. Analysis is provided within the framework of the Manhattan Topology, a multilevel converter topology defined by a set of series stacked capacitors where there exists a scheme to transfer power between capacitors. The differential aspect of this converter comes from the fact that the power exchanged between these capacitors to maintain voltage balance in steady state is less than the total power flow of the converter. The DAHB of the proposed converter is its capacitive power transfer mechanism. A closed-loop control scheme is provided. Lastly, transient and steady-state results of an experimental 1MHz GaN implementation of the proposed topology are shown.

## I. INTRODUCTION

Modular power electronics environments are an area of increasing study [1], [2]. Reconfiguration, through software or hardware, a set of power electronics components for multiple applications has uses ranging from reconfigurable traction inverters [3] to single/three-phase grid-tied inverters [4].

This brief pertains to the series connection of modular power electronics building blocks. A framework for this series connection has been previously derived in [5], [6], denoted the Manhattan Topology, and is defined by a set of series stacked capacitors where each capacitor can share power with others in the stack.

This research brief includes the modeling and control design of a basic 4-capacitor DC/DC configuration of the Manhattan Topology with the capacitive power transfer mechanisms implemented with a Dual-Active-Half-Bridge (DAHB). Nonlinear dynamic equations that describe the system are derived. A feedforward dominated control scheme is designed in conjunction with these equations. Lastly, experimental results showing steady-state and transient performance are provided.

## II. TOPOLOGY

As defined in [6], the Manhattan Topology consists of a set of series stacked capacitors where power can be moved between capacitors. [7], [8] describe different capacitive power transfer connectivities and their functionalities. The configuration of relevance to this research brief is shown in Fig. 1.

The output voltage  $V_o$  is taken at the center of the capacitance stack across  $V_2$  to  $V_0$  in parallel with the load resistance  $R_L$ . The input voltage  $V_s$  is applied across  $V_4$  to  $V_0$ .

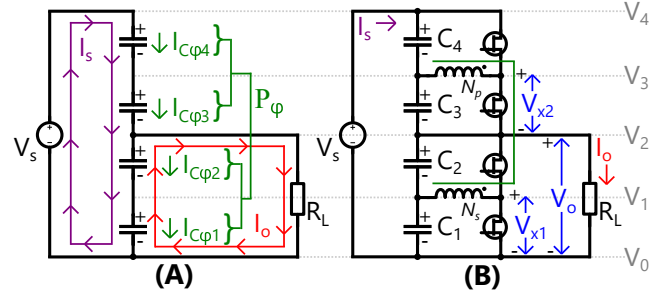


Fig. 1. Topology of the proposed stacked DAHB differential power converter. (A): Capacitor currents and capacitive power transfer scheme. (B): Circuit topology with DAHB capacitive power transfer scheme.

Drawn in Fig. 1-(A) is the converter with the capacitive power transfer mechanisms obfuscated.  $P_\phi$  represents the power transfer over the inductive coupling of the DAHB and is derived from [9]

$$P_\phi = K(V_{C1} + V_{C2})(V_{C3} + V_{C4})\zeta \quad (1a)$$

$$K = \frac{N_p}{N_s 8 f_{sw} L_{lk}} \quad (1b)$$

$$\zeta = \begin{cases} |\phi|(1 - |\phi|) & \text{for } \phi \geq 0 \\ -|\phi|(1 - |\phi|) & \text{for } \phi < 0 \end{cases} \quad (1c)$$

where  $V_{1-4}$  are the voltages of  $C_{1-4}$ ,  $f_{sw}$  is the switching frequency,  $\phi$  is the normalized phase difference between switching cycles of the primary and secondary sides of the DAHB.  $L_{lk}$ ,  $N_p$  and  $N_s$  are the leakage inductance, primary turns number, and secondary turns number, respectively, of the DAHB transformer. As shown in [6], the quantity of power that needs to move from the upper set of capacitors ( $C_3$  and  $C_4$ ) to the lower set of capacitors ( $C_1$  and  $C_2$ ) to maintain capacitor voltage balance is equal to

$$P_{\phi,ss} = P_o \frac{V_s - V_o}{V_s} = P_o \frac{V_{C3} + V_{C4}}{V_{C1} + V_{C2} + V_{C3} + V_{C4}}. \quad (2)$$

As the output voltage  $V_o$  will always be less than the input voltage  $V_s$ , (2) shows that the power required to be moved between capacitors to maintain voltage balance in steady state  $P_{\phi,ss}$  will always be less than the output power  $P_o$ , hence the differential connotation of the proposed.

In the context of this brief, the capacitances values are considered to be equal with  $C = C_1 = C_2 = C_3 = C_4$ .

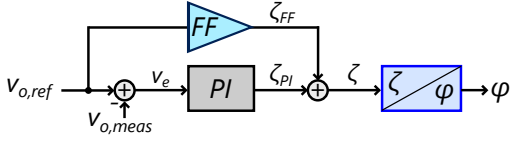


Fig. 2. Control topology of stacked DAHB DC/DC converter.

The duty cycles on both sides of the DAHB are set to always be 0.5. This has the implication that the capacitor voltages and DAHB balancing currents on each side of the DAHB are equal, explicitly written as  $V_{C1} = V_{C2}$ ,  $I_{C\phi1} = I_{C\phi2}$ ,  $V_{C3} = V_{C4}$ , and  $I_{C\phi3} = I_{C\phi4}$ . The individual capacitor currents due to the capacitive power transfer scheme are then

$$I_{C\phi1} = I_{C\phi2} = \frac{1}{C}K(V_{C3} + V_{C4})\zeta \quad (3a)$$

$$I_{C\phi3} = I_{C\phi4} = \frac{1}{C}K(V_{C1} + V_{C2})(-\zeta). \quad (3b)$$

The dynamic equations for the four capacitor voltages can then be found considering  $C(dV_c/dt) = I_c$  and summing the capacitor currents as drawn in Fig. 1-(A) as

$$\frac{dV_{C1}}{dt} = \frac{dV_{C2}}{dt} = \frac{1}{C}K(V_{C3} + V_{C4})\zeta + \frac{1}{C}(I_s - I_o) \quad (4a)$$

$$\frac{dV_{C3}}{dt} = \frac{dV_{C4}}{dt} = \frac{1}{C}K(V_{C1} + V_{C2})(-\zeta) + \frac{1}{C}I_s \quad (4b)$$

where the output current  $I_o$  is equal to  $(V_{C1} + V_{C2})/R_L$ . The input current  $I_s$  can be found considering the law of conservation of energy as

$$I_s = \frac{(V_{C1} + V_{C2})^2}{R_L(V_{C1} + V_{C2} + V_{C3} + V_{C4})}. \quad (5)$$

(4a)-(5) represent a non-linear system with load dependencies. It can be noted that the rightmost terms of (4a)-(4b) are a product of exclusively the load condition, and as  $R_L \rightarrow \infty$  these terms will be driven to zero. If the load parameters are known by the controller then these terms can be artificially driven to zero (for cases of  $R_L \neq \infty$ ) with a feedforward term, as discussed in the following section.

### III. CONTROL

The output voltage of this converter is defined by controlling  $\phi$ .  $\phi$  controls the power flow across the inductive coupling, which is a function of both  $\phi$  and the individual capacitor voltages as described in (1a)-(1c).  $\zeta$  is used as a substitution for the  $\phi$  terms to ease the computational burden. The relationship between  $\phi$  and  $\zeta$  can be found in (1c).

The amount of power that needs to be transferred over the inductive coupling to maintain capacitor voltage balance in steady state can be calculated with (2) if either the load current  $I_o$ , output power  $P_o$ , or load resistance  $R_L$  are known. The feedforward term  $\zeta_{FF}$  can be found by setting (1a) and (2) equal to each other. This results in

$$\zeta_{FF} = \frac{V_{o,ref}}{V_s K R_L} \quad (6)$$

for the case where  $R_L$  is known. When (6) is used as a feedforward term in the control topology shown in Fig. 2, the PI

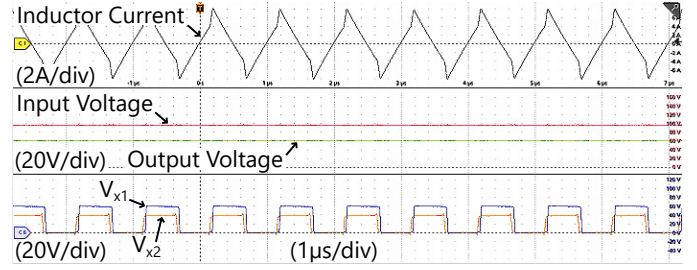


Fig. 3. Steady-state waveforms of the stacked DAHB converter.

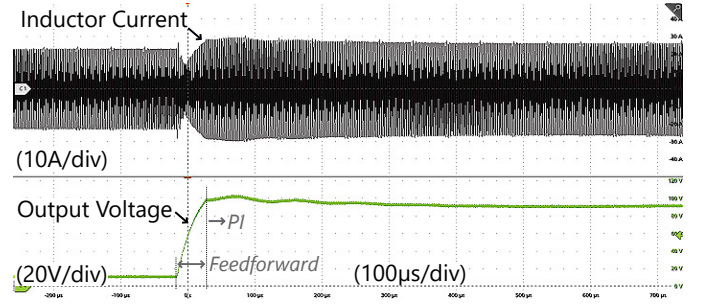


Fig. 4. Transient  $V_o$  step of 10V-90V (10%-90% of  $V_s$ ).

controller only has to control for the first term of (4a)-(4b) and any component nonidealities, eliminating the nonlinearities of (4a)-(4b) introduced by their load dependency. Lastly, using  $\zeta_{FF}$  in (1c), solving the quadratic for  $\phi$ , and bounding  $\phi$  between -0.5 and 0.5 provides the value of  $\phi$  that is used to set the phase difference between opposing sides of the DAHB.

### IV. RESULTS

The circuit of Fig. 1-(B) is implemented in hardware using Texas Instruments LMG3422R030 GaN FETs and a TMS320F28388D microcontroller running with a control frequency of 20kHz. The switching frequency  $f_{sw}$  is 1MHz and the capacitors  $C_{1-4}$  are  $4\mu\text{F}$ . The DAHB transformer is made from two Ferroxcube E43/10/28 3F36 cores with four primary and four secondary turns of 2625/44 Litz wire. The resulting leakage inductance  $L_{lk}$  and magnetization inductance  $L_{mag}$  is  $0.42\mu\text{H}$  and  $65\mu\text{H}$ , respectively. The load resistance  $R_L$  is  $33\Omega$  and the input voltage  $V_s$  is 100V. PI gains of  $k_p = 0.002$  and  $k_i = 20$  are used.

Fig. 3 shows steady state operation with an output voltage  $V_o$  of 60V. The load current is 1.83A, the output power is 110W, and the power transferred between capacitors over the inductive coupling is approximately 44W with a  $\phi$  of 0.065.

Fig. 4 shows a transient  $V_o$  voltage step from 10V to 90V. Minimal overshoot is noted with an initial rise time of approximately  $25\mu\text{s}$ .

### V. CONCLUSION

This brief shows the feasibility of the stacked DAHB implementation of the Manhattan Topology as a DC/DC converter. Functionality and differential power conversion are experimentally validated. Future work involves increasing the number of levels and DC/AC implementation.

## REFERENCES

- [1] Liwei Zhou, Michael Eull, and Matthias Preindl. Optimization-based estimation and model predictive control for high performance, low cost software-defined power electronics. *IEEE Transactions on Power Electronics*, 38(1):1022–1035, 2023.
- [2] Thomas Langbauer, David Menzi, Valentin Marugg, Franz Vollmaier, Jon Azurza, Matthias Kasper, and Johann W. Kolar. Third-harmonic-type modulation minimizing the dc-link energy storage requirement of isolated phase-modular three-phase pfc rectifier systems. *IEEE Access*, 11:34359–34371, 2023.
- [3] Michael Eull, Liwei Zhou, Matthew Jahnes, and Matthias Preindl. Bidirectional nonisolated fast charger integrated in the electric vehicle traction drivetrain. *IEEE Transactions on Transportation Electrification*, 8(1):180–195, 2022.
- [4] Panteleimon Papamanolis, Florian Krismer, and Johann W. Kolar. 22 kw ev battery charger allowing full power delivery in 3-phase as well as 1-phase operation. In *2019 10th International Conference on Power Electronics and ECCE Asia (ICPE 2019 - ECCE Asia)*, pages 1–8, 2019.
- [5] Matthew Jahnes, Bernard Steyaert, and Matthias Preindl. A balanced and vertically stacked multilevel power converter topology with linear component scaling. In *IECON 2021 – 47th Annual Conference of the IEEE Industrial Electronics Society*, pages 1–6, 2021.
- [6] Matthew Jahnes and Matthias Preindl. The manhattan configuration: a differential power converter with linear scaling to n-levels. In *IECON 2022 – 48th Annual Conference of the IEEE Industrial Electronics Society*, pages 1–6, 2022.
- [7] Matthew Jahnes and Matthias Preindl. A family of fully balanced and vertically stacked multilevel power converters with linear scaling. In *2022 IEEE 13th International Symposium on Power Electronics for Distributed Generation Systems (PEDG)*, pages 1–6, 2022.
- [8] Matthew Jahnes and Matthias Preindl. A fully balanced vertically stacked multilevel power converter topology with linear scaling using dual active half bridge converters. In *2022 IEEE Transportation Electrification Conference & Expo (ITEC)*, pages 370–376, 2022.
- [9] Shuai Shao, Linglin Chen, Zhenyu Shan, Fei Gao, Hui Chen, Deshang Sha, and Tomislav Dragičević. Modeling and advanced control of dual-active-bridge dc–dc converters: A review. *IEEE Transactions on Power Electronics*, 37(2):1524–1547, 2022.